Spotlight on Molecular Profiling

Detailed DNA methylation profiles of the E-cadherin promoter in the NCI-60 cancer cells

William C. Reinhold,[1] Mark A. Reimers,[1] Alika K. Maunakea,[1] Sohyoung Kim,[1] Samir Lababidi,[1] Uwe Scherf,[2] Uma T. Shankavaram,[1] Micah S. Ziegler,[1] Claudia Stewart,[3] Hosein Kouros-Mehr,[1] Hengmi Cui,[4] Douglas Dolginow,[2] Dominic A. Scudiero,[3] Yves G. Pommier,[1] David J. Munroe,[3] Andrew P. Feinberg,[4] and John N. Weinstein[1]

[1]Genomics and Bioinformatics Group, Laboratory of Molecular Pharmacology, Center for Cancer Research, National Cancer Institute, NIH, Bethesda, Maryland; [2]Gene Logic, Gaithersburg, Maryland; [3]Science Applications International Corporation-Frederick, Inc., National Cancer Institute at Frederick, Frederick, Maryland; and [4]Epigenetics Unit, Department of Medicine, Johns Hopkins University School of Medicine, Baltimore, Maryland

Abstract

E-cadherin (E-cad) is a transmembrane adhesion glycoprotein, the expression of which is often reduced in invasive or metastatic tumors. To assess E-cad's distribution among different types of cancer cells, we used bisulfite-sequencing for detailed, base-by-base measurement of CpG methylation in E-cad's promoter region in the NCI-60 cell lines. The mean methylation levels of the cell lines were distributed bimodally, with values pushed toward either the high or low end of the methylation scale. The 38 epithelial cell lines showed substantially lower (28%) mean methylation levels compared with the nonepithelial cell lines (58%). The CpG site at -143 with respect to the transcriptional start was commonly methylated at intermediate levels, even in cell lines with low overall DNA methylation. We also profiled the NCI-60 cell lines using Affymetrix U133 microarrays and found E-cad expression to be correlated with E-cad methylation at highly statistically significant levels. Above a threshold of ~20% to 30% mean methylation, the expression of E-cad was effectively silenced. Overall, this study provides a type of detailed analysis of methylation that can also be applied to other cancer-related genes. As has been shown in recent years, DNA methylation status can serve as a biomarker for use in choosing therapy. [Mol Cancer Ther 2007;6(2):391–403]

Introduction

E-cadherin (E-cad) is a transmembrane glycoprotein normally expressed in the plasma membranes of epithelial cells, in which it mediates homophilic, Ca^{2+}-dependent intercellular adhesion in adherens junctions (1). It interacts with the intracellular α, β, and γ catenins (2) and, through those molecules, is connected to the actin cytoskeleton. It acts as a tumor and invasion suppressor (3, 4), the loss of which has been associated with tumorigenesis (5) and increased metastatic potential (6, 7). E-cad is down-regulated in a wide variety of tumors originating from epithelial cells (5, 8–10). Its loss is an indicator of poor prognosis in both breast (11) and prostate (7, 12) cancers.

Multiple mechanisms can reduce E-cad expression. Silencing or reduction of expression has been associated with germ line mutations (13, 14), single nucleotide polymorphisms (15), frame shift and splice site mutations (16, 17), gene deletion (at 16q22.1; ref. 18), and epigenetic events such as histone deacetylation (19), chromatin condensation (20), and promoter region methylation in epithelial tumors (8, 9, 16, 21). Such epigenetic modifications can play important roles in cancer initiation and progression. Those modifications include global or gene-specific promoter region hypomethylation or hypermethylation, chromatin modification, and loss of imprinting (22). Promoter region hypermethylation sometimes provides the ''second hit'' on a remaining intact allele (23) in the context of Knudson's two-hit model of tumor suppressor gene inactivation. E-cad silencing associated with promoter region methylation was first described in gastric cancer (10).

Received 10/3/06; revised 11/27/06; accepted 12/19/06.

Grant support: In part by the Intramural Research Program of the NIH, National Cancer Institute, Center for Cancer Research, and in part by the NCI under contract no. NO1-CO-12400.

The costs of publication of this article were defrayed in part by the payment of page charges. This article must therefore be hereby marked *advertisement* in accordance with 18 U.S.C. Section 1734 solely to indicate this fact.

Requests for reprints: William C. Reinhold, Laboratory of Molecular Pharmacology, Center for Cancer Research, National Cancer Institute, NIH, Building 37, Room 5056, Bethesda, MD 20892-4255. Phone: 301-496-9572; Fax: 301-402-0752. E-mail: wcr@mail.nih.gov

doi:10.1158/1535-7163.MCT-06-0609

The E-cad gene has a CpG island that includes the promoter, exon 1, intron 1, and exon 2 (24). That island is methylated in some epithelial tumors (25). A general association between methylation status and transcript level of E-cad in epithelial tumors has been established for renal (9, 26), bladder (21), and prostate cancers (8). In nonepithelial cell types, the role of E-cad is varied. Glial cells and leukocytes generally do not express E-cad. However, in melanocytes, cell-cell relationships in the skin are determined in part by E-cad (27). In skin, normal melanocytes interact with keratinocytes (28). During the transition to melanoma, E-cad tends to be lost, with concurrent increased expression of N-cadherin, resulting in increased communication between melanoma cells, increased communication between melanocytes and fibroblasts, and loss of association between melanocytes and keratinocytes (28–30).

The current study makes use of the NCI-60 panel that consists of 60 diverse human cancer cell lines which have been used by the National Cancer Institute's Developmental Therapeutics Program to screen and profile >100,000 chemically defined compounds (plus a large number of natural product extracts) since 1990 (31, 32). Included are 38 epithelial and 22 nonepithelial lines derived primarily from patients with advanced and/or metastatic disease. In large part because of the link to molecular pharmacology and drug discovery, the NCI-60 have been more extensively and diversely profiled at the molecular level than any other set of cells in existence (33–40). In November 2006, *Molecular Cancer Therapeutics* launched a new series under the rubric ''Spotlight on Molecular Profiling'' with three articles on molecular characterization of the NCI-60 (41–43).

Here, in the context of the Spotlight series, we present detailed profiles of E-cad methylation in the NCI-60 cell lines obtained by the ''gold-standard'' bisulfite DNA sequencing method. For those studies, we designed PCR primers such that the amplicon would include all 25 CpG sites in the E-cad ''minimal promoter region,'' −191 to +94 bp relative to the transcriptional start (10), plus four additional CpG's at the 3′ end. In addition, we profiled E-cad expression levels in the NCI-60 using Affymetrix U133 microarrays and compared the results with those for E-cad methylation. We were not surprised to find a statistically highly significant negative correlation between the two. We were surprised, however, by the shape of the relationship, which was L-shaped; there seemed to be a ''turn-off'' methylation threshold level of ~20% to 30% above which E-cad expression is essentially abolished.

Materials and Methods

Cell Lines

The NCI-60 cell lines were obtained from the NCI Developmental Therapeutics Program[5] and cultured as described previously (36). Briefly, they were thawed from frozen stocks and cultured in RPMI 1640 (Cambrex, Walkersville, MD) with 5% FCS (Atlantic Biologicals, Norcross, GA) and 2 mmol/L of glutamine (Life Technologies, Inc., Rockville, MD). They were grown to ~80% confluence in T-175 flasks (the last 24 h in fresh medium) before harvest.

RNA and DNA Isolation

RNA was isolated as described previously (36). Briefly, total RNA was purified using the RNeasy purification kit (Qiagen, Inc., Valencia, CA) according to the instructions of the manufacturer. Genomic DNA was purified from cells using the QIAamp DNA Blood Maxi kit (Qiagen) according to the instructions of the manufacturer. Samples were resuspended in 10 mmol/L of Tris and 1 mmol/L of EDTA (pH 8.0). Purified DNA was quantitated by spectrophotometry and aliquoted for storage at −80°C.

U133 Affymetrix Microarray Analysis of Transcript Expression

U133 A and B chips provide analysis of 22,215 features (including ~14,500 known genes) and 22,577 features (including 9,606 known genes), respectively. Robust Multi-chip Analysis was used to process the data. The expression profiling was done in collaboration with U. Scherf, D. Dolginow, and colleagues at Gene Logic, Inc. (Gaithersburg, MD). The methods and the results for all genes on the A-chip are described elsewhere.[6]

Sodium Bisulfite DNA Modification

Genomic DNA (5 μg) from each cell line was treated with sodium bisulfite at 50°C for 17 h using the CpGenome DNA Modification kit from Chemicon International (Temecula, CA) according to the instructions of the manufacturer (except for a 5× volume scale-up through the first washing step on day 2). The DNA was then resuspended in 125 μL of 10 mmol/L Tris with 1 mmol/L of EDTA (pH 7.4; K-D Medical, Columbia, MD). The protocol produced enough material for ~100 PCR sequencing reactions.

PCR Amplification and Sequencing

Nested PCR amplification and sequencing of the DNA were carried out using either converted or unconverted DNA as template for the PCR. Primers were based on the published consensus E-cad promoter DNA sequence (GenBank accession no. L34545). Two pairs of primers were used. For the bisulfite-converted DNA, the first pair consisted of E-cad-nest1 GATTTTAGGTTTTAGTGAGTT upstream (sequence position −397 to −377) and E-cad-nest2/4 GGAAACAGCTATGACCATGAA CTCCAAAA-ACCCATAACTAA downstream (sequence position −6 to +16). These were the outer primers used to anneal and amplify a 413 bp fragment of deaminated DNA in the first round of PCR. The second pair, E-cad-nest3 GTAAAAC-GACGGCCAGTTATTTAGATTTTAGTAATTTT (upstream, sequence position −319 to −299) and E-cad-nest4

[5] See http://dtp.nci.nih.gov/.

[6] U. Shankavaram, W. Reinhold, S. Nishizuka, et al. Transcript and protein expression profiles of the NCI-60 cancer cell panel: an integromic microarray analysis. Mol Cancer Ther 2006. Submitted for publication.

(same as E-cad-nest2) inner primers (with 5′ m13 tails) were then used to amplify a smaller (335 nucleotide) but higher-quality product. For the unconverted DNA, the same locations of primers were used, with E-cad-nest1 GATCCC AGGTCTTAGTGAGCC, E-cad-nest2/4 GGAAACAGC-TATGACCATGTTCTCCAAGGGCCCATG GCTAA, and E-cad-nest3 GTAAAACGACGGCCAGCCACCTAGACCC-TAGCAACTCC. The primers did not contain CpG's and thus would be expected to amplify the DNA without regard to its methylation status. Their design assumed complete C-to-T conversion after bisulfite-treatment. One-strand automated sequencing of the PCR products was done.

Analysis and Visualization of Sequences Using Meth-Miner

Because no available software satisfied our requirement for high-throughput analysis and visualization of the bisulfite sequencing results, we developed the MethMiner program package.[7] MethMiner is a multifunctional tool that (*a*) determines the levels of CpG and non-CpG cytosine methylation, (*b*) incorporates sequence information from nonconverted DNA into the assessment of methylation, (*c*) creates aligned sequence representations, (*d*) creates single-page depictions of CpG and non-CpG methylation patterns, and (*e*) provides numerical representations of methylation status for statistical analysis. MethMiner therefore serves as an aid to the identification of patterns in the many hundreds of sequence reads generated by this project. However, it was not designed to do quality control for automated identification of sequencing errors or mutations, except insofar as they are suggested by visualization of the cytosine by cytosine patterns (see below). We did the essential quality control steps by going manually through each sequence tracing, then comparing the results with those from bisulfite sequencing of corresponding DNA not treated with bisulfite and with the normal human sequence from the Entrez Nucleotide public database.[8]

The input to MethMiner included both chromatograph trace data and sequence information. After multiple alignment of the sequences using Clustal-W (version 1.74) software,[9] and uploading of peak information from the sequence traces, we used MethMiner to analyze the levels of C-to-T conversion [expressed as C / (C + T) ratios] for CpG and non-CpG cytosines. The tracing for each sequencing reaction was inspected visually for obvious flaws, including small peak size, lack of peak separation, and high background. The sequences were sorted first by cell line, then by reaction set. That is, sequence reads were grouped if they had both the same bisulfite conversion date and the same sequencing date. If there were multiple sequencing reads in one of those groups, we calculated a group mean value for each of the 29 CpG methylation levels. The final value for methylation level of a CpG site in a particular cell line was then taken (without correction for incomplete conversion) as the mean of the group mean values. Figure 2 visually indicates the reproducibility of the procedure for a set of reads (38 in all) representing different dates of bisulfite reaction and chromatographic sequencings for one of the cell lines.

Quality Control and Statistical Analyses

In a series of quality control steps, each thymidine/cytosine ratio for each cell line was examined carefully for (*a*) consistency of results from run to run, (*b*) level of non-CpG cytosine conversion (which had to be >90% for acceptance), and (*c*) quality of the original sequence tracings. The fraction for each CpG cytosine was computed as described above. The final methylation values were consistent with results obtained in various laboratories using several different methods: methylation-specific PCR for MCF7, T47D, OVCAR-8/ADR (i.e., NCI-ADR-RES), MDA-MB435, and HL-60 (6, 44, 45); Southern blotting for MCF7 (10); and bisulfite genomic sequencing of cloned DNAs for DU-145, PC-3, CAKI-1, and 786-0 (8, 9). Data in the literature on HS578T indicating high levels of methylation (45) were consistent with our findings because the primers used for methylation-specific PCR coincided with peaks of methylation that we found in the promoter region because of the greater sequence resolution (i.e., base by base) of the bisulfite sequencing methodology (see Table 1; CpG's 7, 8, 16, 22, and 23).

For the correlation of E-cad methylation with transcript levels, we determined 95% confidence intervals by bootstrap with 10,000 resamplings. Unless otherwise stated, all calculations were done using R.[10] Normal, binomial, and bimodal cumulative distribution functions were generated using Excel 2004 for Macintosh (Microsoft, Bellevue, WA).

To test whether different CpG sites showed different distributions of methylation, we applied the Kolmogorov-Smirnov test to each pair of sites. Because many tests were being done in parallel, a multiple-comparisons correction was made. To estimate the joint distribution of Kolmogorov-Smirnov statistics, under the assumption of no differences in distribution, we filled in a 60×29 matrix of values by sampling randomly from the combined distributions of all CpG sites. We then computed the Kolmogorov-Smirnov statistics for all $29 \times 28 / 2$ possible comparisons and saved the maximum of those values. The procedure was repeated 10,000 times to estimate the null distribution of maximal Kolmogorov-Smirnov statistics under the assumption of no differences in distribution.

Results

DNA Methylation Profiles

We used bisulfite sequencing to assess the methylation profiles of E-cad in the NCI-60 cell lines. The mean background level of non-CpG C-to-T conversion after the bisulfite reaction (over all data that passed quality control

[7] S. Kim, manuscript in preparation.
[8] Available from: http://www.ncbi.nlm.nih.gov/entrez/.
[9] Available from: http://molbio.info.nih.gov.
[10] Available from: http://www.r-project.org/.

Table 1. E-cad methylation and expression levels

Cell line†	Percentage of methylation levels (C / C + T) in the NCI-60 cell lines for 29 individual CpG sites of the E-cad promoter region*														
	CpG sites														
	1	2	3	4	5	6	7	8	9	10	11	12	13	14	15
BR:BT-549	22	17	39	37	39	39	49	70	84	60	85	65	78	65	21
BR:HS578T	6	6	5	18	6	63	85	99	99	77	3	1	7	0	5
BR:MCF7	6	9	6	55	6	5	7	4	10	3	29	16	8	12	8
BR:MDA-MB-231	26	30	31	50	3	2	6	8	10	86	14	1	2	4	5
BR:T47D	3	3	3	29	0	2	1	0	3	2	70	0	0	2	6
CNS:SF-268	58	69	59	43	55	49	46	33	28	31	80	51	85	72	25
CNS:SF-295	72	82	76	46	53	47	37	20	17	22	82	59	86	73	28
CNS:SF-539	100	100	87	54	70	54	95	99	81	88	67	26	84	8	12
CNS:SNB19	68	69	81	75	94	95	95	100	100	81	90	70	100	29	77
CNS:SNB-75	11	5	6	45	84	45	70	40	55	14	9	2	11	3	7
CNS:U251	100	92	98	82	91	98	90	98	99	95	100	100	100	24	95
CO:COL0205	1	0	4	42	2	2	4	0	12	4	30	12	1	9	10
CO:HCC-2998	3	0	2	72	3	2	5	2	5	3	10	14	9	5	8
CO:CO-CT-116	2	3	7	44	6	5	4	0	6	10	8	11	5	3	4
CO:HCT-15	5	3	6	27	1	4	1	0	24	2	9	0	2	13	12
CO:HT29	2	0	4	46	5	6	2	1	5	1	13	4	0	8	9
CO:KM12	5	1	5	50	6	3	6	5	8	3	4	0	0	2	8
CO:SW-620	10	5	8	53	30	25	20	10	30	27	60	20	13	13	21
LC:A549-ATCC	17	2	6	35	11	7	5	1	13	10	24	13	8	4	8
LC:EKVX	3	0	2	59	0	0	2	0	6	0	4	7	1	3	7
LC:HOP-62	10	0	35	55	35	10	15	15	10	20	25	20	10	3	18
LC:HOP-92	9	9	6	12	7	5	2	9	7	64	5	7	3	4	5
LC:NCI-H226	4	2	30	12	20	11	17	9	7	2	4	2	3	3	6
LC:NCI-H23	13	11	12	42	3	8	8	2	10	2	39	19	11	5	11
LC:NCI-H322M	2	0	4	42	0	3	1	1	4	0	12	16	0	4	9
LC:NCI-H460	49	47	63	57	55	60	65	50	48	37	41	40	30	26	36
LC:NCI-H522	16	0	28	24	19	19	12	13	27	24	16	55	4	5	7
LE:CCRF-CEM	62	70	88	40	45	52	94	100	98	100	81	75	100	100	84
LE:HL-60	97	95	90	78	94	100	70	64	64	94	84	72	83	41	67
LE:K-562	97	93	94	85	97	97	96	100	100	100	100	100	100	99	95
LE:M0LT-4	92	89	92	100	96	99	96	100	100	92	100	96	100	100	85
LE:RPMI-8226	78	78	71	64	30	29	21	21	14	23	75	19	21	13	13
LE:SR	98	96	100	100	97	90	94	100	99	100	91	96	86	65	96
ME:LOXIMVI	75	73	86	64	84	81	86	97	100	92	96	81	70	38	47
ME:M14	15	0	15	36	20	20	45	7	20	4	22	10	8	17	9
ME:MALME-3M	15	8	16	29	4	7	5	2	15	5	12	7	3	12	7
ME:MDA-MB-435§	57	57	71	49	61	88	64	83	95	100	100	82	100	95	68
ME:MDA-N§	49	56	68	51	39	71	73	89	94	100	100	78	100	87	85
ME:SK-MEL-2	43	41	56	40	27	36	22	22	25	25	36	33	18	23	19
ME:SK-MEL-28	32	35	45	36	33	39	20	20	20	20	38	18	11	20	23
ME:SK-MEL-5	58	53	83	32	81	78	67	78	86	79	85	74	93	54	76
ME:UACC-257	10	0	20	44	0	5	2	0	15	0	10	9	0	10	6
ME:UACC-62	31	42	65	33	62	70	67	41	42	75	71	51	65	11	46
OV:IGROV1	20	6	25	45	33	33	23	24	14	18	47	20	10	2	10
OV:OVCAR-3	6	1	4	53	0	10	2	6	10	1	6	7	10	12	7
OV:OVCAR-4	3	0	3	42	2	1	1	1	10	9	16	5	3	6	8
OV:OVCAR-5	9	4	23	36	11	8	11	8	5	16	64	21	16	2	6

(*Continued on the following page*)

Table 1. E-cad methylation and expression levels (Cont'd)

Percentage of methylation levels (C / C + T) in the NCI-60 cell lines for 29 individual CpG sites of the E-cad promoter region*															Transcript level‡
CpG sites														Mean	
16	17	18	19	20	21	22	23	24	25	26	27	28	29		
17	20	96	49	30	47	53	90	44	92	70	65	98	16	54	4.82
4	9	99	60	0	1	77	100	90	100	99	94	93	60	47	4.91
13	9	57	7	10	10	50	10	5	50	50	44	50	50	21	8.39
1	5	2	0	2	3	0	8	18	3	11	11	13	34	13	4.87
1	4	0	1	2	11	5	5	0	8	11	4	10	1	6	8.46
22	52	90	57	37	33	52	55	32	13	51	24	81	0	48	4.56
13	69	73	35	20	23	40	42	16	0	33	13	58	0	43	4.99
96	95	100	80	77	69	33	99	100	100	97	35	63	57	73	4.85
90	88	100	84	93	90	86	90	98	97	92	89	88	82	86	4.92
3	5	14	0	2	1	0	2	3	13	10	2	5	2	16	4.81
95	95	95	94	93	100	97	98	93	100	89	94	100	90	93	4.83
8	3	8	10	0	10	5	5	5	0	17	2	25	10	8	7.77
7	13	14	8	11	18	13	20	6	8	10	12	26	18	11	26.13
6	13	11	15	12	17	10	9	9	15	10	15	10	0	9	4.97
0	15	29	4	3	20	27	20	13	8	10	7	32	13	11	6.47
8	14	3	9	17	10	10	20	2	18	11	4	11	0	8	6.05
5	6	0	0	2	9	7	10	5	2	4	3	13	6	6	6.33
10	15	90	21	13	37	10	32	5	13	18	3	32	12	23	5.20
0	14	73	19	10	16	18	18	7	20	15	8	15	6	14	5.12
0	12	2	5	5	20	15	17	0	3	12	0	15	0	7	5.58
6	10	86	12	10	0	10	40	10	20	20	20	50	20	21	4.88
1	5	4	0	2	1	1	13	1	3	4	7	3	5	7	4.71
2	8	7	3	1	16	14	13	6	9	96	10	30	6	12	4.86
0	14	26	15	6	10	15	12	10	10	18	13	5	10	12	4.69
0	14	10	14	13	10	15	13	10	15	12	13	25	0	9	6.63
50	69	96	41	41	31	20	25	8	30	34	9	20	22	41	4.90
2	9	10	8	20	24	10	16	14	20	18	0	20	0	15	4.94
100	100	100	98	99	97	94	99	98	100	96	96	100	96	88	4.99
98	89	100	68	94	79	78	100	99	100	89	83	100	84	85	5.24
100	98	100	100	100	100	100	99	99	100	89	100	100	98	98	4.97
100	99	100	100	100	100	100	99	100	100	100	100	100	85	97	5.03
15	10	86	49	21	16	26	58	35	78	50	28	71	23	39	5.06
99	94	100	75	100	96	100	98	99	100	93	97	100	93	95	4.84
92	65	100	98	97	97	98	98	90	100	90	87	100	83	85	4.79
0	15	40	14	8	32	20	20	9	40	50	19	55	8	20	5.03
1	8	7	3	14	17	23	20	3	40	20	8	30	0	12	6.23
100	89	100	89	91	91	85	96	80	100	84	91	100	63	84	5.14
100	89	100	93	99	97	94	93	95	100	89	86	100	77	84	4.80
16	20	45	26	13	18	10	30	22	35	23	13	28	1	26	5.11
10	20	45	30	15	10	10	40	24	50	30	7	30	0	25	4.76
97	76	100	88	84	95	95	89	88	100	90	79	100	65	80	5.23
3	11	6	0	2	10	10	3	0	10	0	0	10	0	7	5.58
64	45	100	79	57	42	75	85	62	100	77	53	94	15	59	4.98
20	17	85	40	15	25	20	20	26	23	22	16	29	10	24	4.93
7	15	20	4	0	5	5	14	3	10	5	0	10	0	8	5.47
0	8	0	6	2	9	7	7	0	0	5	0	0	0	5	5.56
1	6	30	12	7	7	6	2	0	0	8	3	31	11	13	4.81

(*Continued on the following page*)

Table 1. E-cad methylation and expression levels (Cont'd)

Cell line†	Percentage of methylation levels (C / C + T) in the NCI-60 cell lines for 29 individual CpG sites of the E-cad promoter region*														
	CpG sites														
	1	2	3	4	5	6	7	8	9	10	11	12	13	14	15
OV:OVCAR-8	95	87	91	86	91	97	96	98	95	100	100	95	97	70	87
OV:OVCAR-8/ADR§	100	100	100	100	100	100	95	94	100	100	97	100	100	100	4
OV:SKOV3	6	5	10	27	8	5	3	0	8	0	12	7	3	12	9
PR:DU-145	20	24	36	58	15	7	8	5	20	3	10	8	1	10	16
PR:PC-3	2	0	24	45	16	5	8	10	65	15	19	5	13	0	15
RE:786-0	79	74	93	73	86	82	90	99	100	90	95	75	64	43	46
RE:A498	97	90	100	69	100	89	91	93	93	100	98	80	100	35	98
RE:ACHN	15	13	25	36	14	14	14	20	7	11	15	11	9	6	10
RE:CAKI-1	45	60	79	36	53	39	54	19	19	22	14	12	23	8	10
RE:RXF-393	32	32	32	32	9	32	32	5	1	29	45	32	16	1	28
RE:SN12C	62	66	80	58	73	74	69	77	77	89	88	55	76	44	31
RE:TK-10	98	96	100	99	100	98	94	100	100	100	100	100	100	100	99
RE:UO-31	13	6	8	45	11	8	9	5	14	7	10	16	9	12	13
NCI-60 mean	37	35	43	50	38	39	40	38	42	41	48	36	38	28	30
Epithelial mean	24	21	30	47	26	26	27	25	31	30	35	26	22	17	19
Nonepithelial mean	59	57	64	54	57	58	59	58	60	57	66	53	62	45	47
Normality test‖	5.9	6.3	5.3	2.3‖	5.4	5.6	6.2	7.4	7.2	6.8	5.5	5.7	7.9	7.8	8.2

*The last column gives the 29-site mean. Methylation levels calculated as C / (C + T) × 100%. The means of values from multiple experiments when available.
†Tissues of origin: BR, breast; CO, colon; LC, non–small cell lung cancer; LE, leukemia; ME, melanoma; OV ovarian; PR, prostate; RE, renal.
‡Affymetrix fragment name 201130_s_at. Transcript measurement with Gene Logic using U133 microarrays, $\log^2$-transformed. Data processed using the RMA algorithm.
§MDA-MB-435 and MDA-N are considered here to be melanomas; OVCAR-8/ADR is still called NCI/ADR-RES by some, but we have identified it as a derivative of OVCAR-8. See Results for details.
‖−log 10 of the *P* value for the Shapiro-Wilk test of normality (using the R package in Bioconductor). The null hypothesis of normality is strongly rejected for all CpG's, but the value 2.3 (f) indicates that CpG no. 4 is much nearer to normally distributed than are the others.

tests) was 95.4 ± 2.4% (mean ± SD), indicating highly efficient chemical conversion (data not shown). Table 1 presents the percentage of methylation, 100% × C / (C + T), for each of the 29 CpG sites for each of the NCI-60 cell lines, as well as their mean. Included among the NCI-60 are nine tissue-of-origin types: breast (BR), central nervous system glial (CNS), colon (CO), non–small cell lung, ovarian (OV), prostate (PR), and renal (RE) cancers plus leukemias (LE) and melanomas (ME). Overall, the cell lines showed a wide range (from 5% to 99%) of mean methylation levels over the 29 CpG sites. Mean methylation levels for the entire NCI-60, the epithelial cell lines, and the nonepithelial cell lines were 40%, 28%, and 58%, respectively. For the purposes of this study, the cell line MDA-MB435 and its ERBB2-transfectant derivative, MDA-N, were classified as melanomas despite the fact that MDA-MB435 was apparently obtained from the pleural effusion of a patient with breast cancer. MDA-MB435 has been reported to express milk fat proteins and cytokeratin markers characteristic of epithelial cells (46). However, we have found that the two cell lines are extraordinarily similar to the five NCI-60 melanotic melanomas in their profiles of sensitivity to thousands of drugs in the NCI screen (36), their transcript expression profiles (as assessed using six different microarray and RT-PCR platforms; refs. 36, 47–51), and their protein expression profiles as assessed using two-dimensional gels (34) and reverse-phase lysate arrays (52, 53). Independent evidence supporting melanocytic origin has now been presented by others (54). Despite its original classification as MCF7 breast cancer–derived, OVCAR-8/ADR will be considered here as ovarian in origin because of compelling evidence from our karyotypic analyses (35, 55) that it is a (drug-resistant) derivative of OVCAR-8. That conclusion has been corroborated by our gene expression studies and by our analyses of single nucleotide polymorphisms (43).

Figure 1A and B show two visualizations of CpG methylation of the E-cad promoter region. Both visualizations were generated by the MethMiner program package.[7] Figure 1A is a base by base visualization of the methylation status of the NCI-60 for the portion of the promoter that contains CpG site nos. 5 to 10. Those CpG sites appear as the vertical stripes colored according to the figure legend (also see Supplemental Fig. S1 in which

Table 1. E-cad methylation and expression levels (Cont'd)

Percentage of methylation levels (C / C + T) in the NCI-60 cell lines for 29 individual CpG sites of the E-cad promoter region*															Transcript level‡
CpG sites														Mean	
16	17	18	19	20	21	22	23	24	25	26	27	28	29		
90	90	95	75	77	61	76	79	74	96	64	62	88	60	85	4.82
100	2	100	100	99	7	98	99	100	100	100	87	100	100	89	4.96
4	12	10	12	9	5	8	10	5	5	6	5	23	4	8	5.32
11	10	29	3	10	5	5	5	0	25	10	5	32	6	14	5.19
0	6	40	6	10	10	15	20	15	19	11	10	19	0	15	5.21
95	77	100	99	96	95	99	98	96	100	95	91	100	86	87	4.69
96	95	100	100	99	95	95	95	95	100	96	98	100	89	93	4.61
6	4	8	5	1	4	4	3	7	5	7	4	9	6	10	5.01
18	12	93	50	10	22	37	49	10	63	20	27	55	7	33	4.97
1	17	83	24	22	13	9	34	53	60	1	19	NA	8	25	4.73
77	41	100	77	73	74	65	93	94	99	82	84	100	74	74	4.96
100	96	100	99	100	100	100	98	100	100	97	100	100	98	99	5.02
1	16	17	9	8	13	18	10	5	20	18	0	20	0	12	4.70
35	36	57	40	36	36	40	46	38	47	44	36	51	31	40	5.27
20	21	46	27	22	23	28	32	25	33	31	25	38	22	28	5.41
57	58	73	58	57	58	57	65	58	67	62	52	69	46	58	5.03
8.8	7.9	6.9	5.9	7.9	7.3	6.7	6.7	7.7	7.1	6.4	7.3	5.9	7.4	6.5	

the non-CpG converted cytosines appear as vertical strips).[11] In Fig. 1B, the CpG methylation profiles are summarized graphically for all 29 sites sequenced. The technical reproducibility of our bisulfite-sequencing protocol is indicated in Fig. 2. Thirty-eight sequencing reactions from four independent bisulfite conversions, sequenced over a 67-day period, are displayed. The mean SD of the % methylation over the 29 CpG sites is 6.7, and the root mean square error is 7.8.

The Overall Distribution of Methylation Is Bimodal

The overall distribution of cell methylation levels was bimodal, whether viewed at the level of individual CpG sites (except for site no. 4) or as means for the cell lines. Figure 3A shows a histogram of the mean methylation levels of the cell lines (from the second to last column in Table 1). Figure 3B does the same for the 29 × 60 individual CpG sites (Table 1). Figure 3C shows the methylation levels of the 29 CpG sites for the 60 cell lines, sorted in each panel by percentage of methylation. For each CpG except no. 4, the distribution was clearly bimodal, with methylation levels clustering in the range of 0% to 20% or 80% to 100%. Accordingly, as indicated by the last line in Table 1, the Shapiro-Wilk P values for the null hypothesis that the methylation values derived from a normal distribution ranged from 1.5×10^{-9} to 4.9×10^{-3} (i.e., from $-\log(P \text{ value}) = 8.8$ to $-\log(P \text{ value}) = 5.3$ in Table 1, excluding CpG site no. 4). The methylation levels for CpG site no. 4 were more nearly normally distributed, but we can still easily reject the null hypothesis that the distribution is truly normal. The P value was 0.0049 [i.e., $-\log(P \text{ value}) = 2.3$ in Table 1]. The last two panels in Fig. 3C show Qnorm plots for CpG site no. 4, and the mean methylation values visually reflect the difference indicated by the Shapiro-Wilk statistics. If the distribution had been normal, the data points in a Qnorm plot would have lain along the straight, diagonal line. The ''bumps'' above and below the line in the panel for the mean methylation reflect the strikingly bimodal distribution.

The CpG Site 4 Methylation Pattern Is Statistically Different from the Others

Figure 4 shows methylation patterns (see Table 1) for the 60 cell lines across the 29 CpG sites. CpG site no. 4 (cytosine-143 with reference to the transcriptional start site) stood out in that it was more highly methylated, at least in those cell lines with lower overall methylation levels (approximately from BR, HS578T to LE, RPMI-8226). We wondered if that observation could be explained by inefficient bisulfite conversion in that region of the sequence. However, non-CpG cytosines adjacent to site no. 4 (e.g., cytosine-142) showed no drop-off in the conversion to thymidine. Furthermore, the difference was consistent across repetitions. We see nothing unusual about the surrounding sequence that would suggest burial in the secondary or tertiary structure, although that possibility cannot be ruled out formally.

[11] Supplementary material for this article is available at Molecular Cancer Therapeutics Online (http://mct.aacrjournals.org/).

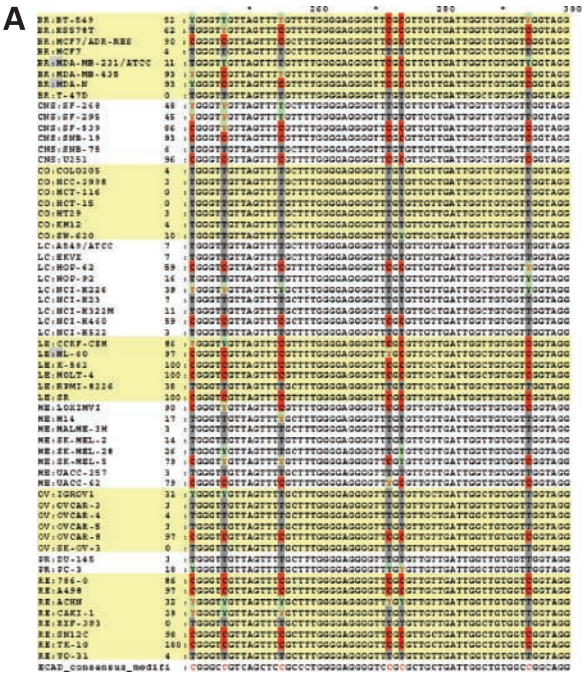

Figure 1. MethMiner graphics indicating the methylation status of CpG sites in the E-cad promoter region for the NCI-60. **A,** MethMiner base by base visualization of the methylation status of the NCI-60. The effects of bisulfite treatment on potential methylation site nos. 5 to 10 appear as vertical colored stripes: *red,* high methylation (C > 66.6%); *green,* partial methylation (C and T each >33.3 but <66.6%); *gray,* low methylation (T > 66.6%). The nine tissue-of-origin types are denoted by the alternating yellow and white regions. *Bottom,* the E-cad (unconverted) reference sequence. **B,** DNA methylation patterns for 29 CpG sites in the E-cad promoter region in the NCI-60 cell lines. *Arrow between sites 15 and 16,* the transcription start site; *ATG,* the translation start codon. *Red points,* 66.7% to 100% methylation; *brown points,* 33.3% to 66.7%; *no points,* 0% to 33.3%. Tissue of origin abbreviations as defined for Table 1. The methylation designation and cell line designation portions of the figure were created using the MethMiner program.[7]

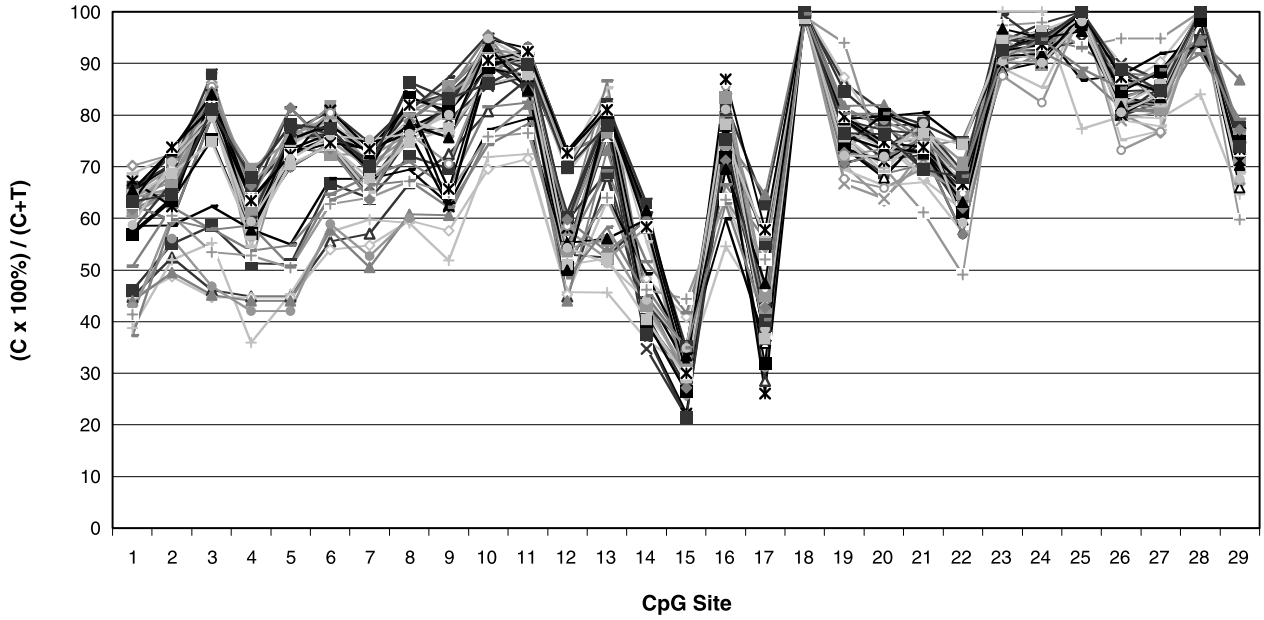

Figure 2. Thirty-eight replicate sequencings of renal cancer SN12C DNA on different dates and with different batches of bisulfite-treatment, demonstrating the reproducibility of the methylation data. C / (C + T) × 100% reflects the percentage of methylation (see text).

To determine whether the pattern of CpG site no. 4 methylation was statistically significant, we used the Kolmogorov-Smirnov test to evaluate the variance of all (29 × 28 / 2) possible CpG site pairings. Only site no. 4 was found to differ from the others in a statistically significant way after multiple comparisons correction. Site nos. 11 and 18 were somewhat similar qualitatively to no. 4 in pattern but not statistically significant in their difference from the rest of the sites.

E-cad Expression Is Correlated with E-cad Methylation and Is Silenced Above ~20% to 30% Methylation

Table 1 presents the E-cad transcript levels as measured by the Affymetrix U133 chip type.[7] The mean methylation and expression patterns for E-cad correlated inversely at statistically significant levels (bootstrap two-tailed $P < 0.05$). Figure 5, which summarizes the comparison of E-cad transcript and methylation patterns, shows an ''L-shaped'' relationship between mean percentage of methylation and mRNA expression. The transcript expression level is undetectable once the methylation level increases to >20% to 30%. When the level of methylation is below that level, the full range of E-cad expression levels is observed. The threshold and L-shape remain clear-cut if E-cad expression is represented on a linear, rather than logarithmic, scale. As we report elsewhere,[12] several other gene expression platforms yield the same L-shaped relationship.

Discussion

In this study, we assessed the promoter region CpG methylation profiles of E-cad across the NCI-60 cell lines, and then correlated the data with E-cad transcript expression. Because it proved almost impossible to analyze the patterns of methylation in that large amount of data (241 interpretable sequences), we developed the MethMiner program package.[7] MethMiner aligns the sequences, produces several different types of color-coded graphics for pattern discernment (e.g., Fig. 1A and B), performs mathematical calculations, and facilitates checks of the four-color sequencer tracings for quality control.

After preliminary analysis of the data, we first asked how mean methylation levels differed from cell type to cell type. The most striking difference was that between epithelial cells (28% on average) and nonepithelial cells (58% on average), presumably reflecting the differences inherent in their normal counterparts. As indicated in Fig. 1B, there were also differences among organs of origin unrelated to the epithelial-nonepithelial dichotomy.

We next analyzed the distribution of methylation across the NCI-60 and found it to be bimodal (at both cell-mean and individual-site levels; Fig. 3A, B, and C). That observation is consistent with the concept that either high or low (but not intermediate) methylation may be the most stable genomic state (56).

We also asked if there were differences among the 29 individual CpG sites in their methylation levels. The answer seems to be yes. CpG site no. 4 (cytosine-143) stands out as being more highly methylated in many of the cell lines that otherwise have moderate to low levels of mean methylation. The Kolmogorov-Smirnov test with multiple comparisons correction yielded a statistically robust difference ($P < 0.05$) in pattern for CpG site no. 4. Cell lines with ≤25% mean methylation (close to the

[12] Reinhold et al., in preparation.

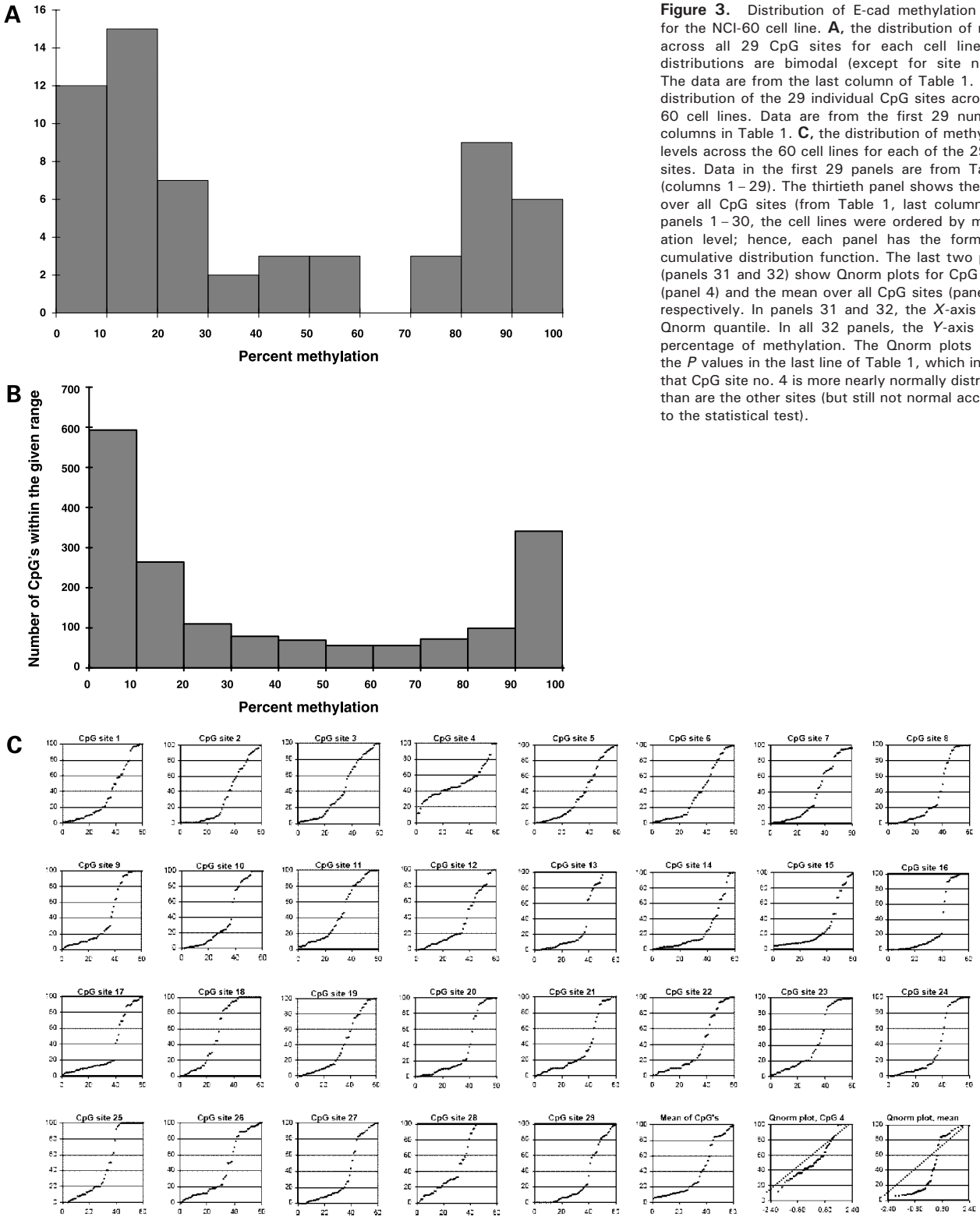

Figure 3. Distribution of E-cad methylation levels for the NCI-60 cell line. **A,** the distribution of means across all 29 CpG sites for each cell line. The distributions are bimodal (except for site no. 4). The data are from the last column of Table 1. **B,** the distribution of the 29 individual CpG sites across the 60 cell lines. Data are from the first 29 numerical columns in Table 1. **C,** the distribution of methylation levels across the 60 cell lines for each of the 29 CpG sites. Data in the first 29 panels are from Table 1 (columns 1 – 29). The thirtieth panel shows the mean over all CpG sites (from Table 1, last column). For panels 1 – 30, the cell lines were ordered by methylation level; hence, each panel has the form of a cumulative distribution function. The last two panels (panels 31 and 32) show Qnorm plots for CpG site 4 (panel 4) and the mean over all CpG sites (panel 30), respectively. In panels 31 and 32, the *X*-axis is the Qnorm quantile. In all 32 panels, the *Y*-axis is the percentage of methylation. The Qnorm plots reflect the *P* values in the last line of Table 1, which indicate that CpG site no. 4 is more nearly normally distributed than are the other sites (but still not normal according to the statistical test).

E-cad expression threshold from Fig. 5) have a mean methylation level of 12.9%, whereas site no. 4 for the same cell lines has a mean of 41.2%, with a *low* value of 12%. The dichotomy becomes even more pronounced for cell lines with the lowest (≤10%) levels of methylation, 9 of 13 of which show measurable E-cad expression levels (Fig. 3). For those cells, an overall mean methylation level of 7.7% contrasts with the site no. 4 mean of 40.5%.

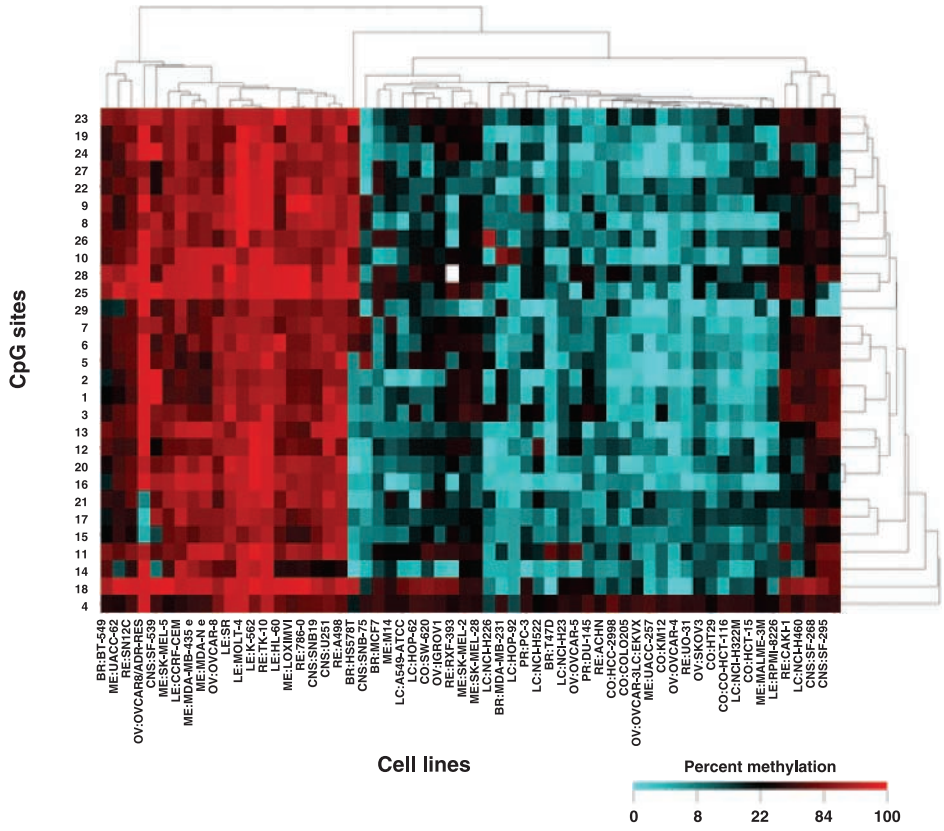

Figure 4. Clustered image map (heat map; ref. 33) of E-cad methylation levels for the 29 CpG sites across the NCI-60. Data are from Table 1. Both axes are clustered based on Euclidian distance using average linkage. The figure was generated using CIMminer; http://discover.nci.nih.gov/cimminer/. The colors are distributed by percentile: *red,* high methylation; *blue,* low methylation.

Those findings are consistent with the concept of a ''seeding'' CpG site for E-cad that is methylated prior to other sites (57, 58), even in the presence of active transcription.

After the foregoing analysis of the methylation patterns themselves, we looked more closely to see how those patterns relate to E-cad transcript expression. Pearson correlation of the mean methylation pattern with E-cad

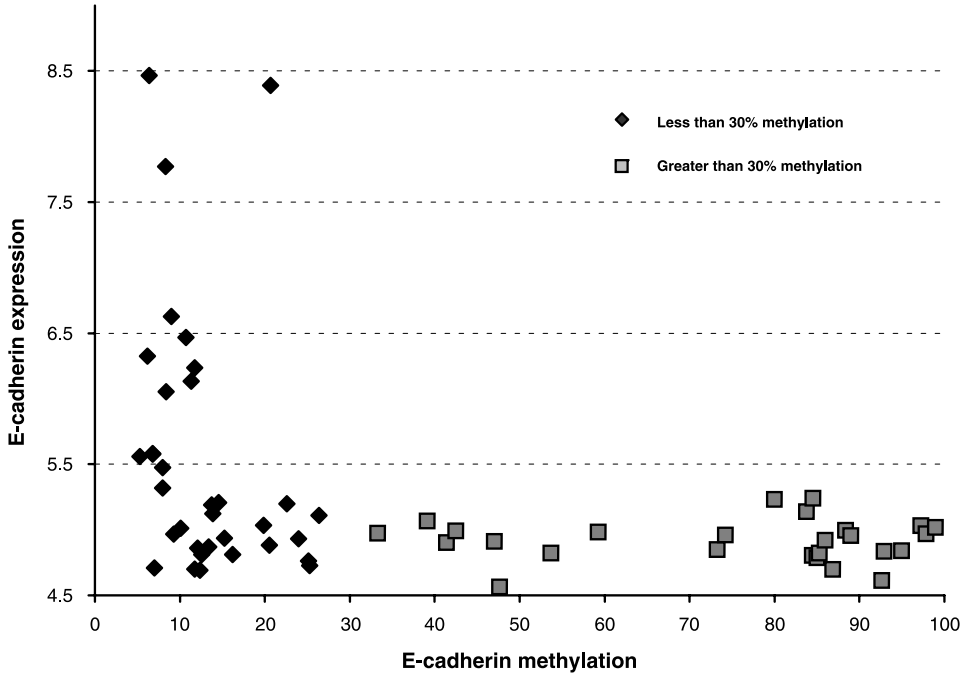

Figure 5. E-cad transcript expression as a function of mean E-cad promoter region methylation for the NCI-60. *Points,* mean expression level across the 29 CpG sites for a single cell line. The data are from Table 1.

transcript expression (Table 1) was quite strongly negative, at −0.38 (bootstrap $P < 0.01$). Because the Pearson correlation coefficient is a measure of linear association, it underestimates the degree of association, given the L-shape of the profile (Fig. 5). The approximately 13 cell lines with detectable E-cad expression (Table 1; Fig. 5) have methylation levels that range from 6% to 21%. E-cad transcript is not detectable in any of the cell lines with higher levels of methylation. Those findings suggest either that active E-cad transcription suppresses more extensive methylation within the promoter or that transcription is strongly inhibited by higher methylation. We had expected the general negative correlation between methylation and expression, in accord with the extensive literature on gene silencing, but the apparent threshold was a surprise.

We next asked whether any of the 29 individual E-cad CpG sites were especially predictive of E-cad expression level. Twenty-eight out of the 29 were statistically significant in their negative correlation with expression, the exception being site no. 4 (data not shown).

The current study doesn't attempt to address the normal versus cancer or normal versus normal question. Rather, we view the current work as a profiling study of E-cad methylation across the NCI-60 cancer cells. Accrual of differences in methylation during carcinogenesis is well accepted in the field, having been studied by several other groups, and documented extensively (5, 6, 8–10, 16, 21, 44, 59).

In conclusion, this review provides a detailed profile of the promoter region methylation status of E-cad in the NCI-60 cell lines and delineates the relationship of that methylation to silencing of the gene. It reports a bimodal distribution of methylation and a major difference in methylation between epithelial and nonepithelial cancer cells types. It also indicates that CpG site no. 4 is partially methylated in cell lines that both transcribe E-cad and have low overall methylation levels, consistent with the idea that site no. 4 is a seed for the methylation process, and perhaps that there is differential methylation of the two DNA strands. Analysis of the association between promoter region methylation and expression of E-cad led to the novel finding of an apparent threshold at ~20% to 30% methylation beyond which E-cad expression is effectively silenced. Based on the results, we have analyzed the relationship of E-cad methylation and expression to the sensitivity of compounds tested in the NCI-60 screen. The results will be presented separately.[13] Overall, this study provides a type of detailed analysis of promoter region methylation that can be applied to additional cancer-related genes. The implications for therapy are clear in that the DNA methylation states of individual genes have proved useful as biomarkers for individualization of therapy (60, 61).

[13] Reinhold et al., manuscript in preparation.

References

1. Overduin M, Harvey T, Bagby S, et al. Solution structure of the epithelial cadherin domain responsible for selective cell adhesion. Science 1995;267:386 – 9.
2. Wijnhoven B, Pignatelli M. E-cadherin-catenin: more than a ''sticky'' molecular complex. Lancet 1999;354:356 – 7.
3. Berx G, Cleton-Jansen A, Nollet F, et al. E-cadherin is a tumour/invasion suppressor gene mutated in human lobular breast cancers. EMBO J 1995;14:6107 – 15.
4. Christofori G, Semb H. The role of the cell-adhesion molecule E-cadherin as a tumour-suppressor gene. Trends Biochem Sci 1999;24:73 – 6.
5. Matsumura T, Makino R, Mitamura K. Frequent down-regulation of E-cadherin by genetic and epigenetic changes in the malignant progression of hepatocellular carcinomas. Clin Cancer Res 2001;7:594 – 9.
6. Nass S, Herman J, Gabrielson E, et al. Aberrant methylation of the estrogen receptor and E-cadherin 5′ CpG islands increases with malignant progression in human breast cancer. Cancer Res 2000;60:4346 – 8.
7. Paul R, Ewing C, Jarrard D, Isaacs W. The cadherin cell-cell adhesion pathway in prostate cancer progression. Br J Urol 1997;79 Suppl 1:37 – 43.
8. Li L, Zhao H, Nakajima K, et al. Methylation of the E-cadherin gene promoter correlates with progression of prostate cancer. J Urol 2001;166:705 – 9.
9. Nojima D, Nakajima K, Li L, et al. CpG methylation of promoter region inactivates E-cadherin gene in renal cell carcinoma. Mol Carcinog 2001;32:19 – 27.
10. Yoshiura K, Kanai Y, Ochiai A, Shimoyama Y, Sugimura T, Hirohashi S. Silencing of the E-cadherin invasion-suppressor gene by CpG methylation in human carcinomas. Proc Natl Acad Sci U S A 1995;92:7416 – 9.
11. Siitonen S, Kononen J, Helin H, Rantala I, Holli K, Isola J. Reduced E-cadherin expression is associated with invasiveness and unfavorable prognosis in breast cancer. Am J Clin Pathol 1996;105:394 – 402.
12. Dunsmuir W, Gillett C, Meyer L, et al. Molecular markers for predicting prostate cancer stage and survival. BJU Int 2000;86:869 – 78.
13. Richards F, McKee S, Rajpar M, et al. Germline E-cadherin gene (CDH1) mutations predispose to familial gastric cancer and colorectal cancer. Hum Mol Genet 1999;8:607 – 10.
14. Sarrio D, Moreno-Bueno G, Hardisson D, et al. Epigenetic and genetic alterations of APC and CDH1 genes in lobular breast cancer: relationships with abnormal E-cadherin and catenin expression and microsatellite instability. Int J Cancer 2003;106:208 – 15.
15. Li L, Chui R, Sasaki M, et al. A single nucleotide polymorphism in the E-cadherin gene promoter alters transcriptional activities. Cancer Res 2000;60:873 – 6.
16. Droufakou S, Deshmane V, Roylance R, Hanby A, Tomlinson I, Hart I. Multiple ways of silencing E-cadherin gene expression in lobular carcinoma of the breast. Int J Cancer 2001;92:404 – 8.
17. Berx G, Becker KF, Hofler H, van Roy F. Mutations of the human E-cadherin (CDH1) gene. Hum Mutat 1998;12:226 – 37.
18. Hiraguri S, Godfrey T, Nakamura H, et al. Mechanisms of inactivation of E-cadherin in breast cancer cell lines. Cancer Res 1998;58:1972 – 7.
19. Peinado H, Ballestar E, Esteller M, Cano A. Snail mediates E-cadherin repression by the recruitment of the Sin3A/histone deacetylase 1 (HDAC1)/HDAC2 complex. Mol Cell Biol 2004;24:306 – 19.
20. Hennig G, Behrens J, Truss M, Frisch S, Reichmann E, Birchmeier W. Progression of carcinoma cells is associated with alterations in chromatin structure and factor binding at the E-cadherin promoter *in vivo*. Oncogene 1995;11:475 – 84.
21. Ribeiro-Filho L, Franks J, Sasaki M, et al. CpG hypermethylation of promoter region and inactivation of E-cadherin gene in human bladder cancer. Mol Carcinog 2002;34:187 – 98.
22. Feinberg A, Tycko B. The history of cancer epigenetics. Nat Rev Cancer 2004;4:143 – 53.
23. Grady W, Willis J, Guilford P, et al. Methylation of the CDH1 promoter as the second genetic hit in hereditary diffuse gastric cancer. Nat Genet 2000;26:16 – 7.
24. Berx G, Staes K, van Hengel J, et al. Cloning and characterization of the human invasion suppressor gene E-cadherin (CDH1). Genomics 1995;26:281 – 9.

25. Esteller M, Corn P, Baylin S, Herman J. A Gene Hypermethylation Profile of Human Cancer. Cancer Res 2001;61:3225 – 9.

26. Kawakami T, Okamoto K, Ogawa O, Okada Y. Multipoint methylation and expression analysis of tumor suppressor genes in human renal cancer cells. Urology 2003;61:226 – 30.

27. Herlyn M, Berking C, Li G, Satyamoorthy K. Lessons from melanocyte development for understanding the biological events in naevus and melanoma formation. Melanoma Res 2000;10:303 – 12.

28. Hsu M, Andl T, Li G, Meinkoth J, Herlyn M. Cadherin repertoire determines partner-specific gap junctional communication during melanoma progression. J Cell Sci 2000;113:1535 – 42.

29. Li G, Fukunaga M, Herlyn M. Reversal of melanocytic malignancy by keratinocytes is an E-cadherin-mediated process overriding β-catenin signaling. Exp Cell Res 2004;297:142 – 51.

30. McGary E, Lev D, Bar-Eli M. Cellular adhesion pathways and metastatic potential of human melanoma. Cancer Biol Ther 2002;1:459 – 65.

31. Paull K, Shoemaker R, Hodes L, et al. Display and analysis of patterns of differential activity of drugs against human tumor cell lines: development of mean graph and COMPARE algorithm. J Natl Cancer Inst 1989; 81:1088 – 92.

32. Boyd M. Status of the NCI preclinical antitumor drug discovery screen. In Cancer: principles and practice of oncology update. Vol. 3. Philadelphia: J.B. Lippincott; 1989.

33. Weinstein J, Myers T, O'Connor P, et al. An information-intensive approach to the molecular pharmacology of cancer. Science 1997;275: 343 – 9.

34. Myers T, Anderson N, Waltham M, et al. A protein expression database for the molecular pharmacology of cancer. Electrophoresis 1997; 18:647 – 53.

35. Roschke A, Tonon G, Gehlhaus K, et al. Karyotypic complexity of the NCI-60 drug-screening panel. Cancer Res 2003;63:8634 – 47.

36. Scherf U, Ross D, Waltham M, et al. A gene expression database for the molecular pharmacology of cancer. Nat Genet 2000;24:236 – 44.

37. Stinson S, Alley M, Kopp W, et al. Morphological and immunocytochemical characteristics of human tumor cell lines for use in a disease-oriented anticancer drug screen. Anticancer Res 1992;12:1035 – 53.

38. Holbeck S. Update on NCI *in vitro* drug screen utilities. Eur J Cancer 2004;40:785 – 93.

39. Weinstein J. Integromic Analysis of the NCI-60 Cancer, Cell Lines. Breast Dis 2004;19:11 – 22.

40. Izquierdo M, Shoemaker R, Flens M, et al. Overlapping phenotypes of multidrug resistance among panels of human cancer-cell lines. Int J Cancer 1996;65:230 – 7.

41. Weinstein J. Spotlight on molecular profiling: 'integromic' analysis of the NCI-60 cancer cell lines. Mol Cancer Ther 2006;5:2601 – 5.

42. Lorenzi P, Reinhold W, Rudelius M, et al. Asparagine synthetase as a causal, predictive biomarker for L-asparaginase activity in ovarian cancer cells. Mol Cancer Ther 2006;5:2613 – 23.

43. Ikediobi O, Davies H, Bignell G, et al. Mutation analysis of twenty-four known cancer genes in the NCI-60 cell line set. Mol Cancer Ther 2006;5: 2606 – 12.

44. Corn P, Smith B, Ruckdeschel E, Douglas D, Baylin S, Herman J. E-cadherin expression is silenced by 5′ CpG island methylation in acute leukemia. Clin Cancer Res 2000;6:4243 – 8.

45. Graff JR, Herman JG, Myohanen S, Baylin SB, Vertino PM. Mapping patterns of CpG island methylation in normal and neoplastic cells implicates both upstream and downstream regions in *de novo* methylation. J Biol Chem 1997;272:22322 – 9.

46. Sellappan S, Grijalva R, Zhou X, et al. Lineage infidelity of MDA-MB-435 cells: expression of melanocyte proteins in a breast cancer cell line. Cancer Res 2004;64:3479 – 85.

47. Ross D, Scherf U, Eisen M, et al. Systematic variation in gene expression patterns in human cancer cell lines. Nat Genet 2000;24: 227 – 35.

48. Staunton J, Slonim D, Coller H, et al. Chemosensitivity prediction by transcriptional profiling. Proc Natl Acad Sci U S A 2001;98:10787 – 92.

49. Szakacs G, Annereau J, Lababidi S, et al. Predicting drug sensitivity and resistance: profiling ABC transporter genes in cancer cells. Cancer Cell 2004;6:129 – 37.

50. Huang Y, Anderle P, Bussey K, et al. Membrane transporters and channels: role of the transportome in cancer chemosensitivity and chemoresistance. Cancer Res 2004;64:4294 – 301.

51. Annereau J, Szakacs G, Tucker CJ, et al. Analysis of ATP-binding cassette transporter expression in drug-selected cell lines by a microarray dedicated to multidrug resistance. Mol Pharmacol 2004;66:1397 – 405.

52. Nishizuka S, Charboneau L, Young L, et al. Proteomic profiling of the NCI60 cancer cell lines using new high-density 'reverse-phase' lysate microarrays. Proc Natl Acad Sci U S A 2003;100:14229 – 34.

53. Nishizuka S, Chen S, Gwadry F, et al. Diagnostic markers that distinguish colon and ovarian adenocarcinomas: identification by genomic, proteomic, and tissue array profiling. Cancer Res 2003;63:5243 – 50.

54. Ellison G, Klinowska T, Westwood R, Docter E, French T, Fox J. Further evidence to support the melanocytic origin of MDA-MB-435. Mol Pathol 2002;55:294 – 9.

55. Bussey KJ, Chin K, Lababidi S, et al. Integrating data on DNA copy number with gene expression levels and drug sensitivities in the NCI-60 cell line panel. Mol Cancer Ther 2006;5:853 – 67.

56. Rakyan V, Hildmann T, Novik K, et al. DNA methylation profiling of the human major histocompatibility complex: a pilot study for the human epigenome project. PLos Biol 2004;2:e405.

57. Clark S, Melki J. DNA methylation and gene silencing in cancer: which is the guilty party? Oncogene 2002;21:5380 – 7.

58. Stirzaker C, Song J, Davidson B, Clark S. Transcriptional gene silencing promotes DNA hypermethylation through a sequential change in chromatin modifications in cancer cells. Cancer Res 2004;64: 3871 – 7.

59. Graff JR, Gabrielson E, Fujii H, Baylin SB, Herman JG. Methylation patterns of the E-cadherin 5′ CpG island are unstable and reflect the dynamic, heterogeneous loss of E-cadherin expression during metastatic progression. J Biol Chem 2000;275:2727 – 32.

60. Esteller M, Garcia-Foncillas J, Andion E, et al. Inactivation of the DNA-repair gene MGMT and the clinical response of gliomas to alkylating agents. N Engl J Med 2000;343:1350 – 4.

61. Weinstein J. Pharmacogenomics—teaching old drugs new tricks. N Engl J Med 2000;343:1350 – 4.